



Cite this: *Chem. Commun.*, 2015, 51, 7827

Received 11th March 2015,  
Accepted 2nd April 2015

DOI: 10.1039/c5cc02059j

[www.rsc.org/chemcomm](http://www.rsc.org/chemcomm)

**Fluorescence microscopy studies using 4-morpholinoscriptaid (4MS) demonstrated rapid cellular uptake of this scriptaid analogue into the cytoplasm but no nuclear penetration. As 4MS and scriptaid have the same *in vitro* activity against HDACs and KASUMI-1 cells; 4MS exemplifies a rational approach to subtly modify 'profluorogenic' substrates for intracellular studies.**

Fluorescent tagging of bioactives for cell based microscopy studies is conventionally achieved by conjugating, by means of a spacer, a bulky fluorophore to the drug of interest.<sup>1</sup> While fluorescent, the extraneous conjugation to a fluorophore invariably leads to an increase in molecular weight and has an impact on *c log P*—parameters that medicinal chemists spend considerable effort optimising. Indeed, the behaviour of the 'tagged' compound in cells might not accurately reflect that of the parent.

Ideally, only subtle structural modifications would be performed on a bioactive to render it fluorescent. Despite the seemingly obvious benefits of such an approach, no examples could be found.<sup>‡</sup> While this strategy is limited somewhat in that only aromatic compounds can be considered, the dominance of highly aromatic scaffolds in drug discovery makes it complementary to the conventional 'tagging' approach. A bioactive that is identified as being structurally related to an existing fluorophore might be termed 'profluorogenic'; for example naphthalene is a common component of biologically active compounds<sup>2</sup> and is the core of several highly fluorescent entities including the 4-aminonaphthalimides.<sup>3</sup>

<sup>a</sup> Research Centre for Chemistry and Biotechnology, School of Life and Environmental Sciences, Deakin University, Waurn Ponds, Victoria, 3216, Australia. E-mail: fred.pfeffer@deakin.edu.au

<sup>b</sup> Monash Institute of Pharmaceutical Science, Royal Parade, Parkville, Victoria, 3052, Australia

<sup>c</sup> Peter MacCallum Cancer Centre, St Andrews Place, East Melbourne, Victoria, 3002, Australia

† Electronic supplementary information (ESI) available: Detailed experimental procedures, <sup>1</sup>H NMR and <sup>13</sup>C NMR spectra of compounds, as well as photophysical results are provided. See DOI: 10.1039/c5cc02059j

## A fluorescent histone deacetylase (HDAC) inhibitor for cellular imaging<sup>†</sup>

Cassandra L. Fleming,<sup>a</sup> Trent D. Ashton,<sup>a</sup> Cameron Nowell,<sup>b</sup> Mark Devlin,<sup>c</sup> Anthony Natoli,<sup>c</sup> Jeannette Schreuders<sup>c</sup> and Frederick M. Pfeffer<sup>a\*</sup>

Scriptaid (**1**, Fig. 1) is a well-studied histone deacetylase (HDAC) inhibitor with established anticancer activity.<sup>4,5</sup> More recently, scriptaid (**1**) has also been shown to have beneficial effects in the treatment of HIV and neurodegenerative disorders.<sup>6</sup> Scriptaid (**1**) possesses the typical pharmacophore of HDAC inhibitors which includes (i) zinc binding group (chelates the Zn<sup>2+</sup> ion of the active site, see Fig. 1) (ii) linker (occupies a hydrophobic tunnel) which connects to the (iii) capping group (solvent exposed).<sup>7</sup>

Recognising the structural similarities of the 4-amino-1,8-naphthalimide fluorophore and the known HDAC inhibitor scriptaid (**1**), the fluorescent scriptaid analogue **4MS** was developed (Fig. 1); the key feature being the introduction of the relatively small 4-morpholino substituent (*M<sub>W</sub>* = 87).

While SAR studies of scriptaid do not extend to modifications of the capping group, we reasoned that, given the non-critical role of the capping group with respect to HDAC inhibition, introduction of a small amino moiety would not have deleterious effects on HDAC activity. Indeed, calculated properties (*c log P* and PSA) of scriptaid (**1**) and **4MS** showed only subtle differences (see ESI<sup>†</sup> for full details) and thus it was anticipated that other than fluorescence, **4MS** would behave in a near identical fashion to the parent.

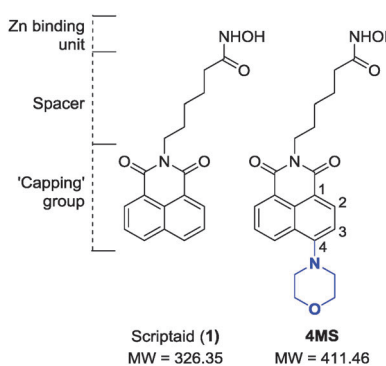
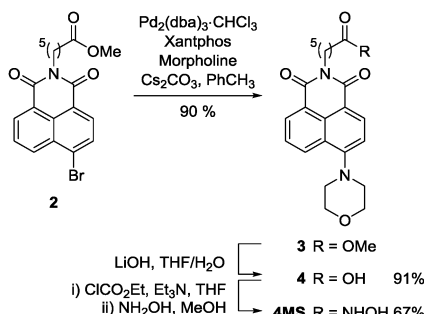


Fig. 1 Structure of scriptaid (**1**) and the fluorescent **4MS**. Regions of the HDAC pharmacophore are also indicated.

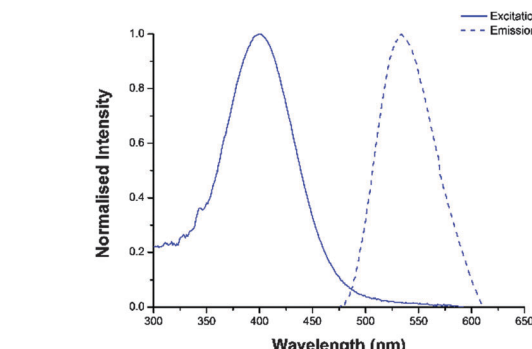
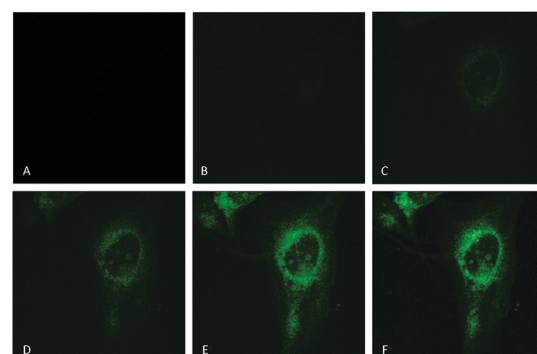


Scheme 1 Synthesis of **4MS**.

To construct **4MS**, 4-bromonaphthalimide **2** (see ESI† for synthesis) was converted to the corresponding 4-morpholino derivative **3** using a palladium mediated Buchwald–Hartwig approach (Scheme 1).<sup>8</sup> Treatment of 4-bromonaphthalimide **3** with morpholine (3 equiv.),  $\text{Pd}_2(\text{dba})_3 \cdot \text{CHCl}_3$  (4 mol%) and the commercially available ligand, Xantphos (4 mol%) in the presence of  $\text{Cs}_2\text{CO}_3$  (3 equiv.) at 40 °C for 24 h gave the desired aryl amine **3** in excellent yield (90%). Carboxylic acid **4** was obtained in high yield (91%) using excess LiOH·H<sub>2</sub>O. The free acid was converted to the mixed anhydride (using  $\text{ClCO}_2\text{Et}$  and  $\text{Et}_3\text{N}$ ) then *in situ* treated with hydroxylamine (in methanol) to give the desired hydroxamic acid **4MS** in good yield (67%, 50% over 4 steps).

Compound **4MS** was then assessed for inhibitory activity against HDAC isoforms 1, 3 and 8 (class I), 6 (class IIb) and HDAC 11 (class IV). The introduction of the morpholine group was not deleterious towards HDAC inhibition. Indeed, when compared to scriptaid (**1**), **4MS** had similar activity against both HDAC6 ( $\text{IC}_{50} = 12 \text{ nM}$ , Table 1) and HDAC3 (**4MS**,  $\text{IC}_{50} = 0.32 \mu\text{M}$ ; *cf.* **1**,  $\text{IC}_{50} = 0.37 \mu\text{M}$ ) and was slightly more efficacious against HDAC1 ( $\text{IC}_{50} = 1.43 \mu\text{M}$ ) than scriptaid (**1**,  $\text{IC}_{50} = 1.74 \mu\text{M}$ ). As such, **4MS** displayed a similar selectivity profile to that of scriptaid (**1**) for HDAC6 over HDAC1 and HDAC3. For the other class I isoform investigated (HDAC8) **4MS** inhibited with an  $\text{IC}_{50}$  of 1.81  $\mu\text{M}$  compared with 1.52  $\mu\text{M}$  for **1** which corresponds to improved selectivity (**4MS**, SF = 151; *cf.* **1**, SF = 127). A moderate improvement in activity was also obtained at HDAC11 (**4MS**,  $\text{IC}_{50} = 0.29 \mu\text{M}$ ; *cf.* **1**,  $\text{IC}_{50} = 0.36 \mu\text{M}$ ).

Both scriptaid (**1**) and **4MS** exhibit modest selectivity towards HDAC6, which is known to modulate a number of cytosolic processes that can lead to cell stress and apoptosis including  $\alpha$ -tubulin deacetylation and binding to the stress granule protein, G3PB1.<sup>9</sup> Indeed, HDAC6 inhibitors have been proposed as therapies for acute myeloid leukemia,<sup>10</sup> a hematological cancer represented by KASUMI-1 cells. As such the ability of **4MS** to

Fig. 2 Normalised excitation and emission spectra of **4MS** in DMSO.Fig. 3 Confocal microscopy images of MDA-MB-231 cells showing the rapid cellular uptake of **4MS** at 1.0  $\mu\text{M}$ . Images are of the following time points: (A) 0 s, (B) 10 s, (C) 20 s, (D) 30 s, (E) 40 s, (F) 50 s.

decrease cell growth was evaluated in KASUMI-1 cells (Table 1) and **4MS** inhibited the growth of the leukemia cell line with an  $\text{IC}_{50}$  of 0.29  $\mu\text{M}$ , which is comparable with scriptaid (**1**,  $\text{IC}_{50} = 0.49 \mu\text{M}$ ).

The photophysical properties of **4MS** were typical of 4-dialkylamino-1,8-naphthalimide derivatives<sup>11</sup> and proved to be well suited for fluorescence microscopy. In DMSO, the absorption maximum (Fig. 2) was 399 nm with an emission maximum at 534 nm (Stokes shift = 135 nm). This compares favourably with scriptaid (**1**), which presents no visible fluorescence.

To demonstrate the potential of **4MS** as a tool to provide pharmacokinetic information, confocal microscopy was used to visualise the cellular penetration and subcellular location of **4MS** in the human breast cancer MDA-MB-231 cell line. The cells were treated *in situ* with a 1.0  $\mu\text{M}$  solution of **4MS** and images were taken at 10 second time points (Fig. 3A–F). At each time point, a significant increase in emission intensity from the treated cells was evident, clearly indicating rapid cellular uptake.

Table 1 Inhibition of individual HDAC isoforms,  $\text{IC}_{50}$  ( $\mu\text{M}$ )

Compound	HDAC isoform (SF), SF = selectivity factor vs. HDAC6					KASUMI-1
	1	3	6	8	11	
Scriptaid ( <b>1</b> )	$1.74 \pm 0.06^a$ (145)	$0.37 \pm 0.06$ (31)	$0.012 \pm 0.0026$	$1.52 \pm 0.01$ (127)	$0.36 \pm 0.03$ (30)	$0.49^b$
<b>4MS</b>	$1.43 \pm 0.13$ (119)	$0.32 \pm 0.04$ (27)	$0.012 \pm 0.0019$	$1.81 \pm 0.17$ (151)	$0.29 \pm 0.02$ (24)	0.29

<sup>a</sup> Values represent the average of two measurements ( $n = 2$ ). <sup>b</sup> Error < 1% ( $n = 3$ ).

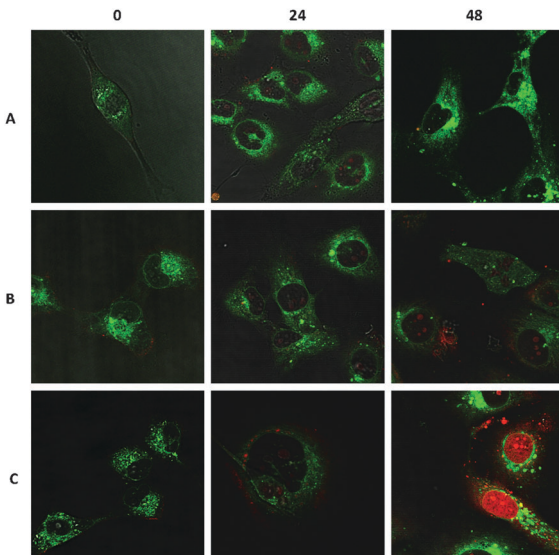


Fig. 4 Confocal microscopy images of **4MS** within MDA-MB-231 cells at (A) 0.025  $\mu$ M, (B) 0.1  $\mu$ M, (C) 0.3  $\mu$ M. Cells were co-stained with propidium iodide to monitor cell death and fluorescent images were taken at the following time points: 0, 24 and 48 h. Green = **4MS**. Red = propidium iodide.

Cellular uptake of biologically active molecules is currently generally monitored by radio-labelling or fluorescent tagging.<sup>12</sup> While radio-labelling can be achieved through isotopic replacement it requires specialised equipment and precautions. As mentioned, fluorescent tagging often leads to a significant increase in the molecular weight of the known biologically active compound. Large increases in molecular weights may result in poor absorption and cell permeation of the fluorescent therapeutic.<sup>13</sup> By utilising the inherent fluorescent properties of **4MS**, rapid cellular uptake was visualised in less than 50 seconds.

Additional time course studies were conducted at lower concentrations (0.025–0.30  $\mu$ M), in which **4MS** was incubated in MDA-MB-231 cells for 48 h and co-stained with propidium iodide to monitor cell death (Fig. 4). No fluorescence was observed in the nucleus, suggesting that **4MS** did not penetrate the nuclear envelope. It is possible that the lack of observed fluorescence in the nucleus was due to DNA mediated fluorescence quenching rather than lack of penetration therefore titrations of **4MS** with calf thymus (*ct*)-DNA were conducted. While a slight decrease in the emission intensity of **4MS** was observed upon the addition of *ct*-DNA in phosphate buffer (10 mM at pH 7.4), the emission band of **4MS** was still clearly visible after a large excess of *ct*-DNA had been added (see ESI†). These results indicate that **4MS** was not entering the nucleus and that the lack of fluorescence emission from the nucleus was not a result of DNA binding/quenching. The observed cytoplasmic accumulation is interesting given the concentration of HDACs in the nucleus and may ultimately prove advantageous as the class II HDAC isoforms, such as HDAC6, are known to shuttle between the nucleus and the cytoplasm and mediate processes such as  $\alpha$ -tubulin deacetylation.<sup>14</sup>

Based on our results, it might be possible to design selective inhibitors for class II HDAC by refining the localisation profile of the therapeutic rather than focussing solely on enhancing its specific enzyme binding.

Upon incubation of MDA-MB-231 cells with the fluorescent **4MS** at 0.025 and 0.1  $\mu$ M no significant changes were observed (Fig. 4A and B, respectively). However, the treatment of MDA-MB-231 cells with 0.3  $\mu$ M **4MS**, cell death was evident within 48 h (Fig. 4C).

In summary, the rational design and synthesis of **4MS** has been performed. Structural changes from scriptaid (**1**) were minimal and were not detrimental to isoform selectivity or anticancer activity (KASUMI-1). The strategic location of the morpholino substituent at the 4-position of the naphthalimide imparted photophysical properties and enabled the study of these compounds in cells using fluorescence microscopy; demonstrated with the visualisation of rapid cellular uptake and subsequent distribution in MDA-MB-231 cells. This fluorescent analogue has very quickly contributed to our understanding of how the well-studied scriptaid (**1**) acts at a cellular level and is likely to be a value to the many researchers currently investigating scriptaid (**1**) as a potential neuroprotectant and anticancer agent.

CLF thanks the Research Centre for Chemistry and Biotechnology for a top-up scholarship. The authors would like to acknowledge the Australian Research Council for funding Deakin University's Nuclear Magnetic Resonance Facility through LIEF grant LE110100141, as well as for additional equipment support related to this project (LE120100213).

## Notes and references

‡ A comprehensive literature search involving combinations of keywords including "theranostics", "fluorescent drugs", "tagging" and "bioactive" gave no relevant results.

- (a) T. Liu, L. Y. Wu, M. Kazak and C. E. Berkman, *Prostate*, 2008, **68**, 995; (b) E. L. Ricket, S. Oriana, C. Hartman-Frey, X. Long, T. T. Web, K. P. Nephew and R. V. Weatherman, *Bioconjugate Chem.*, 2010, **21**, 903.
- (a) J. D. Durrant, L. Hall, R. V. Swift, M. Landon, A. Schnaufer and R. E. Amaro, *PLoS Neglected Trop. Dis.*, 2010, **4**, e803; (b) R. S. Upadhyaya, J. K. Vandavasi, R. A. Kardile, S. V. Lahore, S. S. Dixit, H. S. Deokar, P. D. Shinde, M. P. Sarmah and J. Chattopadhyaya, *Eur. J. Med. Chem.*, 2010, **45**, 1854.
- (a) D. Esteban-Gómez, L. Fabbrizzi and M. Licchelli, *J. Org. Chem.*, 2005, **70**, 5717; (b) E. B. Veale and T. Gunnlaugsson, *J. Org. Chem.*, 2008, **73**, 8073; (c) R. Parkesh, T. C. Lee and T. Gunnlaugsson, *Tetrahedron Lett.*, 2009, **50**, 4114.
- (a) L. Giacinti, C. Giacinti, C. Gabellini, E. Rizzuto, M. Lopez and A. Giordano, *J. Cell. Physiol.*, 2012, **227**, 3426; (b) E. J. Lee, B. B. Lee, S. J. Kim, Y. D. Park, J. Park and D. H. Kim, *Int. J. Oncol.*, 2008, **33**, 767; (c) N. Takai, T. Ueda, M. Nishida, K. Nasu and H. Narahara, *Int. J. Mol. Med.*, 2006, **17**, 323.
- The inhibition of HDAC enzymes has proven to be a valuable therapeutic tool for the treatment of various disease states including cyclic fibrosis, type II diabetes, neurodegenerative disorders and cancer. For examples refer to: (a) D. M. Hutt, C. A. Olsen, C. J. Vickers, D. Herman, M. A. Chalfant, A. Montero, L. J. Leman, R. Burkle, B. E. Maryanoff, W. E. Balch and M. R. Ghadiri, *ACS Med. Chem. Lett.*, 2011, **2**, 703; (b) D. P. Christensen, M. Dahlöf, M. Lundh, D. N. Rasmussen, M. D. Nielsen, N. Billestrup, L. G. Grunnet and T. Mandrup-Poulsen, *Mol. Med.*, 2011, **17**, 378; (c) A. G. Kazantsev and L. M. Thompson, *Nat. Rev. Drug Discovery*, 2008, **7**, 854; (d) C. M. Marson, *Anti-Cancer Agents Med. Chem.*, 2009, **9**, 661; (e) R. W. Johnstone, *Nat. Rev. Drug Discovery*, 2002, **1**, 287.



6 (a) K. Huber, G. Doyon, J. Plaks, E. Fyne, J. W. Mellors and N. Sluis-Cremer, *J. Biol. Chem.*, 2011, **286**, 22211; (b) G. Wang, X. Jiang, H. Pu, W. Zhang, C. An, X. Hu, A. K. Liou, R. K. Leak, Y. Gao and J. Chen, *Neurotherapeutics*, 2013, **10**, 124.

7 T. A. Miller, D. J. Witter and S. Belvedere, *J. Med. Chem.*, 2003, **46**, 5097.

8 C. L. Fleming, T. D. Ashton and F. M. Pfeffer, *Dyes Pigm.*, 2014, **109**, 135.

9 (a) Y. Gao, C. C. Hubbert, J. Lu, Y. Lee, J. Lee and T. Yao, *Mol. Cell. Biol.*, 2007, **27**, 8637; (b) S. Kwon, Y. Zhang and P. Matthias, *Genes Dev.*, 2007, **21**, 3381.

10 B. Hackanson, L. Rimmele, M. Benkiser, M. Abdelkarim, M. Fliegauf, M. Jung and M. Lübbert, *Leuk. Res.*, 2012, **36**, 1055.

11 (a) S. Banerjee, E. B. Veale, C. M. Phelan, S. A. Murphy, G. M. Tocci, L. J. Gillespie, D. O. Frimannsson, J. M. Kelly and T. Gunnlaugsson, *Chem. Soc. Rev.*, 2013, **42**, 1601.

12 X. Chu, K. Korzekwa, R. Elsby, K. Fenner, A. Galetin, Y. Lai, P. Matsson, A. Moss, S. Nagar, G. R. Rosania, J. P. F. Bai, J. W. Polli, Y. Sugiyama and K. L. R. Brouwer, *Clin. Pharmacol. Ther.*, 2013, **94**, 126.

13 R. B. Silverman, in *The Organic Chemistry of Drug Design and Drug Action*, Elsevier Science, Burlington, 2nd edn, 2004, ch. 2, p. 65.

14 G. I. Aldana-Masangkay and K. M. Sakamoto, *J. Biomed. Biotechnol.*, 2010, **2011**, 1.

